Journal of Crystal Growth 323 (2011) 450–453

Contents lists available at ScienceDirect

Journal of Crystal Growth

journal homepage: www.elsevier.com/locate/jcrysgro

Quantum dot lasers grown by gas source molecular-beam epitaxy

Q. Gong [a],*, P. Chen [a], S.G. Li [a], Y.F. Lao [a], C.F. Cao [a], C.F. Xu [a], Y.G. Zhang [a], S.L. Feng [a], C.H. Ma [b], H.L. Wang [b]

[a] *State Key Laboratory of Functional Materials for Informatics, Shanghai Institute of Microsystem and Information Technology, Chinese Academy of Sciences, 865 Changning Road, Shanghai 200050, People's Republic of China*

[b] *College of Physics and Engineering, Qufu Normal University, Qufu 273165, People's Republic of China*

ARTICLE INFO

Available online 10 December 2010

Keywords:
B3. Quantum dot lasers
A3. Gas source molecular-beam epitaxy
B2. InAs
B2. InP
B2. GaAs
B3. Semiconductor lasers

ABSTRACT

We report on the InAs quantum dot lasers grown by gas source molecular-beam epitaxy, respectively, on GaAs and InP substrates. Room temperature continuous-wave operation was achieved for both InAs/GaAs and InAs/InP quantum dot lasers, respectively, at 1.10 μm and 1.54−1.70 μm wavelength region. More than 50 mW optical power was collected from one facet of the InAs/GaAs quantum dot lasers at 20 °C, while for InAs/InP quantum dot lasers the maximum output power was measured as 30 mW. For InAs/InP material system, by increasing the layer thickness of deposited InAs from 3.0 to 3.5 monolayers, the lasing wavelength can be extended from 1.5−1.6 μm to 1.6−1.7 μm. Moreover, a tunable quantum dot external cavity laser was demonstrated, utilizing the broad gain profile of InAs quantum dots.

1. Introduction

InAs quantum dots (QDs) have been extensively studied as the active material of high performance QD lasers [1–4]. Successful growth of InAs QD lasers has been achieved in variant techniques such as solid-state molecular-beam epitaxy (SSMBE) [5–8], metal organic vapor-phase epitaxy (MOVPE) [9–13], chemical-beam epitaxy [14], and gas source molecular-beam epitaxy (GSMBE) [15–18]. In particular, GSMBE takes advantage of SSMBE while utilizing well-developed high temperature injectors for arsenic and phosphorus sources. Thus, GSMBE is capable of growing both GaAs-based and InP-based semiconductor structures with control of layer thickness and interface as precise as SSMBE. In this paper, we studied the InAs QD lasers grown by GSMBE, respectively, on GaAs and InP substrates. Good laser performances have been obtained from the laser diodes grown by GSMBE. Moreover, a InAs/GaAs QD laser diode was placed inside an external cavity in Littrow configuration. A tuning range of 38 nm was obtained while the threshold current density was kept below 1 kA/cm^2 in the full tuning range. For InAs/GaAs QD lasers, we explored the possibility of gain broadening by growing the active region with InAs layers of different thicknesses. On the other hand, for InAs/InP QD lasers, it was demonstrated that the lasing wavelength can be extended from 1.5−1.6 μm to 1.6−1.7 μm by increasing the thickness of InAs layer for QD formation from 3.0 to 3.5 monolayers (MLs). Because the lattice misfit between InAs and GaAs is much larger than that between InAs and InP, InAs QDs formed on GaAs are smaller than that on InGaAsP/InP. In addition, the barrier materials for InAs/GaAs QDs are different from the InAs/InGaAsP/InP ones. Thus, different regions of emission wavelength are usually covered by the InAs/GaAs QDs (1.0−1.4 μm) and InAs/InGaAsP/InP QDs (1.5−1.7 μm), respectively.

2. Growth and device fabrication

The samples were grown, respectively, on n-type GaAs and InP (1 0 0) substrates by GSMBE, where III-element flux is produced from pure metal gallium, indium, and aluminum. Arsenic and phosphorus fluxes are produced by introducing AH_3 and PH_3 gas through a high temperature injector at 1000 °C. Note that the V-element flux is always accompanied by a hydrogen flux resulted from the thermal decomposition of introduced hydrides. After thermally removing the native oxide layer on the substrate, QD laser structures were grown with detailed structures described below. Ridge waveguide laser diodes were fabricated with strip width of 6 μm. The Fabry–Perot (FP) cavity was formed by the cleaved facet without coating. The output power was measured by a Melles Griot optical power meter including an integrating sphere Ge detector. Lasing spectra were recorded by a Fourier transform infrared spectrometer equipped with a InSb detector with resolution of 0.125 cm^{-1}. All the measurements were carried out in CW mode and a heating stage was used for temperature dependent measurements in the range of 20–80 °C.

3. Results and discussions

3.1. InAs/InP QD lasers

The grown InAs/InP QD laser structure consists of 600 nm 1×10^{18} cm^{-3} Si-doped InP buffer layer, 100 nm InGaAsP ($\lambda_g = 1.18$ μm)

---

* Corresponding author.
E-mail address: qgong@mail.sim.ac.cn (Q. Gong).

0022-0248/$ - see front matter © 2010 Elsevier B.V. All rights reserved.
doi:10.1016/j.jcrysgro.2010.12.014

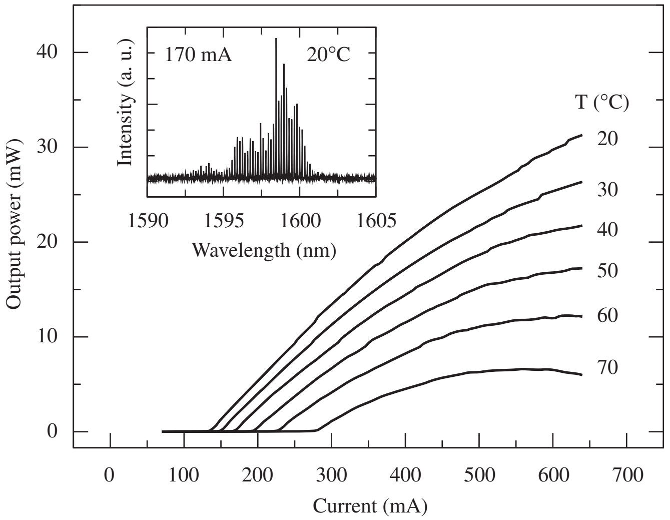

Fig. 1. Output power vs injection current of InAs/InP QD laser under CW operation in the temperature range of 20–70 °C. The QD layer was formed by 3.0 MLs InAs. Inset is the lasing spectrum taken at 20 °C.

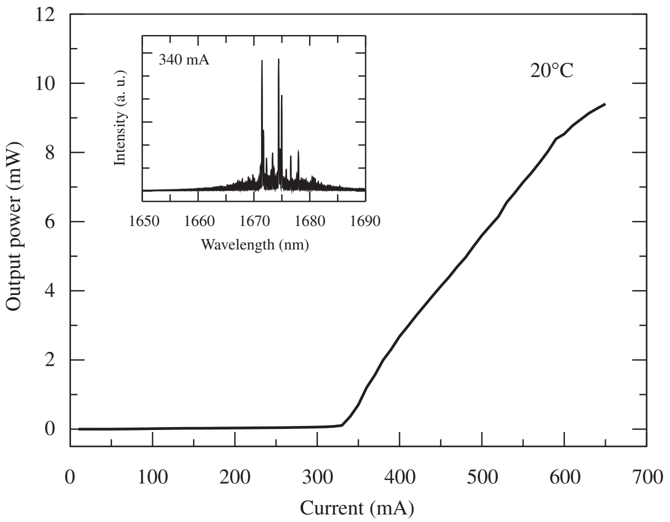

Fig. 2. Output power vs injection current of InAs/InP QD laser under CW operation at 20 °C. The QD layer was formed by 3.5 MLs InAs. Inset is the lasing spectrum.

layer, five-stacked InAs QD layers separated by 40 nm InGaAsP ($\lambda_g = 1.18$ µm) spacers, 100 nm InGaAsP ($\lambda_g = 1.18$ µm) layer, 1.5 µm 5×10^{17} cm^{-3} Be-doped InP layer, and 200 nm Be-doped InGaAs layer. The QD layer was formed by 3.0 MLs InAs. The active region was grown at 485 °C and the InP layers were grown at 465 °C. The QDs were found to be round and slightly elongated along the $[0\,1\,\bar{1}]$ direction, with mean dot height of 2.9 nm and mean base diameter of 76 nm [18]. For another sample, 3.5 MLs InAs layer was deposited to form the QD layer.

For the laser structure with QD layer formed by 3.0 MLs InAs, the light output characteristics of the QD laser were shown in Fig. 1 for a 2.0 mm-long laser diode. At 20 °C, the threshold current density was measured as 1.1 kA/cm^2. From one facet more than 30 mW optical power was collected. The lasing spectrum centered at 1598 nm is shown in the inset of Fig. 1 for a laser diode driven by 170 mA at 20 °C. The maximum output power dropped gradually to about 5mW when the heat sink was raised to 70 °C. By the temperature dependence of the threshold current, the characteristic temperature of the QD laser diode was derived as 69 K. By reducing the cavity length of the QD laser, shorter lasing wavelength was observed. Because the mirror loss rises with decrease in the cavity length, resulting in shorter lasing wavelength where the gain is high enough for lasing [18].

It is found that the lasing wavelength of QD lasers can be extended by depositing more InAs to form the QD layer. The lasing wavelength was shifted into the range of $1.6-1.7$ µm when the QD layer was formed by 3.5 MLs InAs. The output power vs injection current at 20 °C is shown in Fig. 2 for a 1.5 mm-long laser diode, with threshold current density of 3.7 kA/cm^2. The maximum output power per facet was measured as about 10 mW. The lasing wavelength is around 1.67 µm, as shown in the inset of Fig. 2 when the diode was driven by 340 mA. Obviously the laser performances were degraded by the increase in the layer thickness of InAs deposited for the QD layer. It is likely that the thickness of 3.5 MLs is too thick to keep the QD layer defect free.

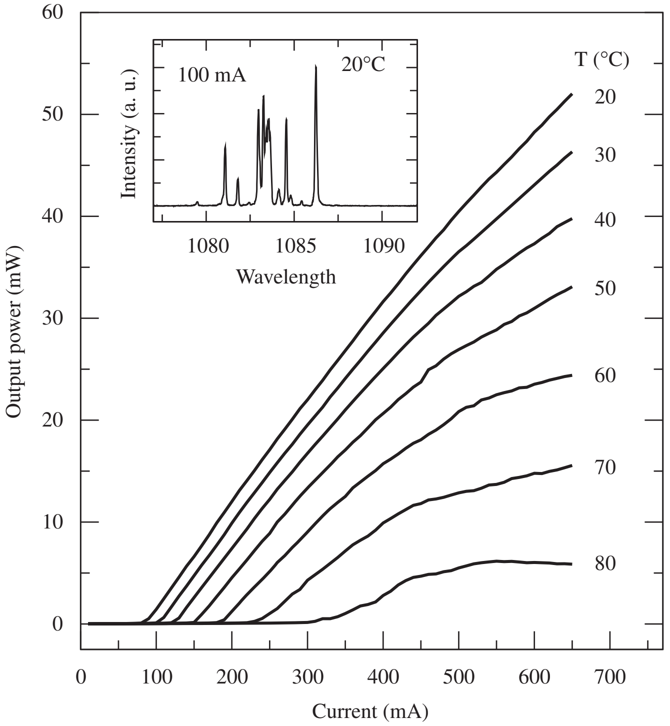

Fig. 3. Output power vs injection current of InAs/GaAs QD laser under CW operation in the temperature range of 20–80 °C. Inset is the lasing spectrum taken at 20 °C.

3.2. *InAs/GaAs QD lasers*

The grown structure of InAs/GaAs QD lasers consists of 500 nm 2×10^{18} cm^{-3} Si-doped GaAs buffer layer, 1.5 µm 1×10^{18} cm^{-3} Si-doped $Al_{0.3}Ga_{0.7}As$ layer, 80 nm thick undoped $Al_{0.15}Ga_{0.85}As$ layer, the active region, 80 nm thick undoped $Al_{0.15}Ga_{0.85}As$ layer, 1.5 µm 1×10^{18} cm^{-3} Be-doped $Al_{0.3}Ga_{0.7}As$ layer, and 200 nm Be-doped GaAs contact layer. The core active region includes five-stacked InAs QD layers, respectively, formed by 2.3, 2.4, 2.5, 2.6, and 2.7 MLs InAs. The QD layers were grown at 500 °C and separated by 40 nm GaAs spacer. The GaAs buffer and AlGaAs layers were grown at 580 °C. It is expected that different thicknesses of deposited InAs layer might result in broad size distribution of InAs QDs. Broad gain profile, thus, can be achieved, which is of great importance for broadly tunable lasers.

The dependence of output power on injection current is shown in Fig. 3 at varying heat sink temperatures for a 2.5 mm-long laser diode. At 20 °C, the threshold current density was 615 A/cm^2, and more than 50 mW optical power was measured in CW mode from

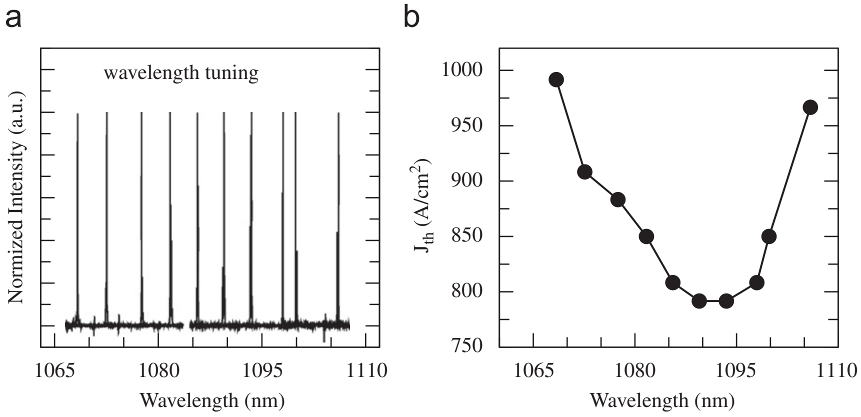

Fig. 4. (a) Lasing spectra of the InAs/GaAs QD external cavity laser tuned by rotating the grating in Littrow configuration. (b) The threshold current density vs the lasing wavelength.

one facet. The lasing spectrum centered at 1083 nm is shown in the inset of Fig. 3 for the laser diode driven by 100 mA at 20 °C. The threshold current increases with the heat sink temperature. However, CW operation was maintained up to 80 °C and 6 mW maximum optical power was recorded at 80 °C. The lasing wavelength can be selected in the range of $1.05-1.10$ μm by cleaving the diodes into different cavity length, due to the same mechanism discussed above for InP-based QD lasers. From the dependence of external quantum efficiency on the cavity length, the internal quantum efficiency was derived as 30.5% and the internal lose as 3.7 cm^{-1}. In the temperature range of 20–80 °C, the characteristic temperature (T_0) of the laser threshold current was deduced as 49 K from the measured $L-I$ data shown in Fig. 3.

3.3. Tunable QD external cavity lasers

Since QD lasers have potential application in low-threshold tunable external cavity laser with very wide tunable range [19], we placed the InAs/GaAs QD laser diode inside an external cavity in Littrow configuration. The results are shown in Fig. 4. By varying the angle of grating the lasing wavelength can be tuned in the range of 1068–1106 nm, as shown in Fig. 4(a). Note that during the full range of wavelength tuning, the threshold current was below 1 kA/cm^2, as shown in Fig. 4(b). Although wide tuning range of 38 nm has been achieved, its potential for widely tunable laser has not been fully explored. One of the key points is that the tested laser diode has no facet coating, which prevents the diode lasing from excited states. Lasing from the ground state easily occurs between the cleaved facets when the injection current is raised. Therefore, the tuning range is expected to be drastically enlarged by applying anti-reflection layer to one of the cleaved facet.

4. Conclusion

We have investigated the InAs quantum dot lasers grown by gas source molecular-beam epitaxy on, respectively, GaAs and InP substrates. For GaAs based QD lasers, CW operation has been achieved at temperatures up to 80 °C and more than 50 mW output optical power was measured from one facet at 20 °C. The lasing wavelength is around 1.1 μm. For InP based QD lasers, the maximum output power at 20 °C was measured as 30 mW and CW operation was kept up to 70 °C. Lasing wavelength of QD lasers can be extended by increasing the layer thickness of InAs. In addition, we studied the tunable InAs/GaAs QD external cavity laser in Littrow configuration and tuning range of 38 nm was obtained. In the full tuning range the threshold current density was kept below 1 kA/cm^2. Thus, much wider tuning range is expected when an anti-reflection layer is applying to one of the laser facet, which allow the external cavity laser working under larger injection currents.

Acknowledgement

This work was supported by the National Natural Foundation of China (Grant nos. 60576009, 60721004, and 60976015).

References

[1] D.L. Huffaker, G. Park, Z. Zou, O.B. Shchekin, D.G. Deppe, 1.3 μm room-temperature GaAs-based quantum-dot laser, Appl. Phys. Lett. 73 (18) (1998) 2564–2566.

[2] M. Grundmann, The present status of quantum dot lasers, Physica E 5 (2000) 167–184.

[3] Z. Mi, P. Bhattacharya, S. Fathpour, High-speed 1.3 μm tunnel injection quantum-dot lasers, Appl. Phys. Lett. 86 (15) (2005) 153109.

[4] C.S. Lee, W. Guo, D. Basu, P. Bhattacharya, High performance tunnel injection quantum dot comb laser, Appl. Phys. Lett. 96 (10) (2010) 101107.

[5] P.B. Joyce, T.J. Krzyzewski, P.H. Steans, G.R. Bell, J.H. Neave, T.S. Jones, Variations in critical coverage for InAs/GaAs quantum dot formation in bilayer structures, J. Cryst. Growth 244 (2002) 39–48.

[6] Q.H. Xie, A. Madhukar, P. Chen, N.P. Kobayashi, Vertically self-organized InAs quantum box islands on GaAs (100), Phys. Rev. Lett. 75 (13) (1995) 2542–2545.

[7] J.M. Garcia, G. Medeiros-Ribeiro, K. Schmidt, T. Ngo, J.L. Feng, A. Lorke, J. Kotthaus, P.M. Petroff, Intermixing and shape changes during the formation of InAs self-assembled quantum dots, Appl. Phys. Lett. 71 (4) (1997) 2014–2016.

[8] J.S. Kim, J.H. Lee, S.U. Hong, W.S. Han, H.-S. Kwack, C.W. Lee, D.K. Oh, Room-temperature operation of InP-based InAs quantum dot laser, IEEE Photon. Technol. Lett. 16 (7) (2004) 1607–1609.

[9] J. Oshinowo, M. Nishioka, S. Ishida, Y. Arakawa, Highly uniform InGaAs/GaAs quantum dots (15 nm) by metalorganic chemical vapor deposition, Appl. Phys. Lett. 65 (11) (1994) 1421–1423.

[10] F. Heinrichsdorff, A. Krost, M. Grundmann, D. Bimberg, A. Kosogov, P. Werner, Self-organization processes of InGaAs/GaAs quantum dots grown by metalorganic chemical vapor deposition, Appl. Phys. Lett. 68 (23) (1996) 3284–3286.

[11] F. Heinrichsdorff, M.H. Mao, N. Kirstaedter, A. Krost, D. Bimberg, A.O. Kosogov, P. Werner, Room-temperature continuous-wave lasing from stacked InAs/GaAs quantum dots grown by metalorganic chemical vapor deposition, Appl. Phys. Lett. 71 (1) (1997) 22–24.

[12] J.W. Jang, S.H. Ryun, S.H. Lee, I.C. Lee, W.G. Jeong, R. Stevenson, P. Daniel Dapkus, N.J. Kim, M.S. Hwang, D. Lee, Room temperature operation of InGaAs/InGaAsP/InP quantum dot lasers, Appl. Phys. Lett. 85 (17) (2004) 3675–3677.

[13] S. Anantathanasarn, R. Nötzel, P.J. van Veldhoven, F.W.M. van Otten, Y. Barbarin, G. Servanton, T. de Vries, E. Smalbrugge, E.J. Geluk, T.J. Eijkemans, E.A.J.M. Bente, Y.S. Oei, M.K. Smit, J.H. Wolter, Lasing of wavelength-tunable (1.55 μm region) InAs/InGaAsP/InP(1 0 0) quantum dots grown by metal organic vapor-phase epitaxy, Appl. Phys. Lett. 89 (2006) 073115.

[14] P.J. Poole, K. Kaminska, P. Barrios, Z. Lu, J. Liu, Growth of InAs/InP-based quantum dots for 1.55 μm laser applications, J. Cryst. Growth 311 (2009) 1482–1486.

[15] F.Y. Chang, C.C. Wu, H.H. Lin, Effect of ingaas capping layer on the properties of InAs/InGaAs quantum dots and lasers, Appl. Phys. Lett. 82 (25) (2003) 4477–4479.

[16] C. Paranthoen, N. Bertru, O. Dehaese, A. Le Corre, S. Loualiche, B. Lambert, G. Patriarche, Height dispersion control of InAs/InP quantum dots emitting at 1.55 μm, Appl. Phys. Lett. 78 (12) (2001) 1751–1753.

[17] F. Lelarge, B. Rousseau, B. Dagens, F. Poingt, F. Pommereau, A. Accard, Room temperature continuous-wave operation of buried ridge stripe lasers using InAs-InP (1 0 0) quantum dots as active core, IEEE Photon. Technol. Lett. 17 (7) (2005) 1369–1371.

[18] S.G. Li, Q. Gong, Y.F. Lao, K. He, J. Li, Y.G. Zhang, S.L. Feng, H.L. Wang, Room temperature continuous-wave operation of InAs/InP(1 0 0) quantum dot lasers grown by gas-source molecular-beam epitaxy, Appl. Phys. Lett. 93 (11) (2008) 111109.

[19] P.M. Varangis, H. Li, G.T. Liu, T.C. Newell, A. Stintz, B. Fuchs, K.J. Malloy, L.F. Lester, Low-threshold quantum dot lasers with 201 nm tuning range, Electron. Lett. 36 (18) (2000) 1544–1545.